MULTI-SCALE LINE DETECTION FOR LANDSLIDE FISSURE MAPPING

André Stumpf [a, b, c], *Thomas A. Lampert* [d], *Jean-Philippe Malet* [b], *Norman Kerle* [c]

[a] Laboratoire Image, Ville, Environnement, CNRS ERL 7230, Université de Strasbourg, 3 rue de l'Argonne, F- 67083 Strasbourg, France
[b] Institut de Physique du Globe de Strasbourg, CNRS UMR 7516, Université de Strasbourg / EOST, 5 rue René Descartes, F-67084 Strasbourg, France
[c] ITC-Faculty of Geo-Information Science and Earth Observation, University of Twente, Department of Earth Systems Analysis, Hengelosestraat 99, P.O. Box 6, Enschede, 7500 AA, The Netherlands
[d] Image Sciences, Computer Sciences and Remote Sensing Laboratory, CNRS UMR 7005, Université de Strasbourg, Bd Sébastien Brant, BP 10413, F-67412 Illkirch, France

ABSTRACT

Surface fissures are important indicators for slope instability and their patterns reveal information about the distribution of strain and mechanical processes. The increasing availability of sub-decimeter resolution aerial images may enable the detection and mapping of such features with imagery. This study combines Gaussian matched filters and first order derivates in a multi-scale framework to address the semi-automatic detection of surface cracks with variable sizes. The accuracy of the detector was assessed with two expert mappings and compared to a corresponding single scale approach.

Index Terms—surface cracks, landslide, unmanned aerial vehicles, matched filters

1. INTRODUCTION

Surface discontinuities observed in rocks and sediments have proven to be valuable indicators of the deformation history and stress pattern of slopes. For landslide analysis, their observation and interpretation can contribute to a better understanding of the controlling physical processes and help in the assessment of the related hazards [1, 2]. Surface fissures may indicate the development of future failures [3-5] and are often considered as a geo-indicator of the landslide activity stage. In sediments, the surface fissure characteristics also influence water infiltration and drainage, which in turn affect the ground-water system and the kinematic response of slopes to hydrological events [6].

Recent studies [7] have shown that VHR images acquired from Unmanned Aerial Vehicles (UAVs) are cost-efficient data sources for the monitoring of landslide surfaces at spatial resolutions that allow the recognition of surface features at sub-decimeter scale. Although the detection and extraction of linear features is a fundamental operation in digital image processing [8, 9], relatively few studies have explored the application of automatic approaches for the mapping of such features [10-13].
Therefore, this study targeted the development of a largely automated image analysis technique to detect landslide surface fissures from VHR aerial images. The developed method is based on scalable Gaussian directional filters that can be used at a single scale or with combined responses over multiple scales. The approach was tested on a VHR image acquired at the Super-Sauze landslide in the Southeast French Alps, and the obtained results were compared to manual mappings carried out by experts.

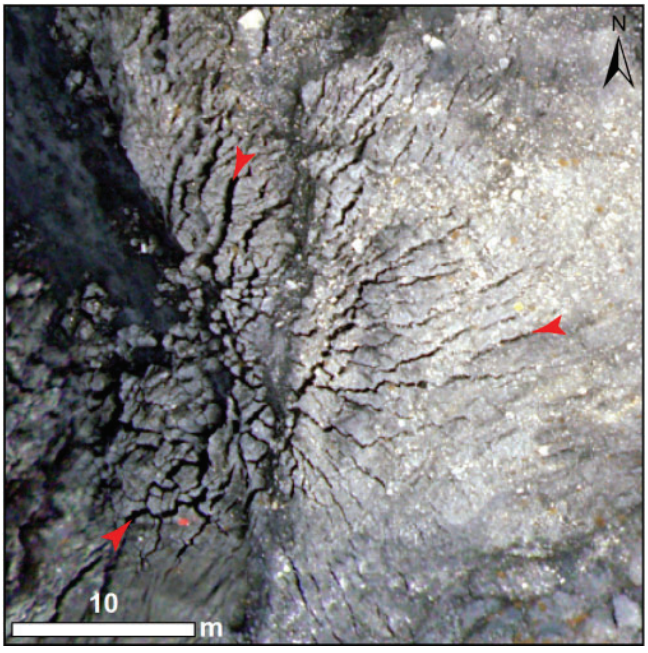

Fig. 1 Test subset of the UAV image with fissures of different sizes marked exemplarily (red arrows).

2. DATA AND METHOD

The study site is the slow-moving Super-Sauze landslide located in the Southern French Alps. In October 2010, Niethammer et al. conducted an aerial survey using a UAV system at flight heights between 100 and 250 m, resulting in imagery with a spatial resolution of 0.08 m. The image acquisition and processing is detailed in [7]. For this study 35 × 35 m subset of the image was adopted, and the results of the automatic detection were compared with fissure maps elaborated by two experts.

The fissures appear as dark curvy-linear features that are 1–10 pixels wide and feature cross-profiles that resemble an inverted Gaussian function. Following earlier works that exploited such properties for the detection of retinal blood vessels [14, 15], a detection routine using a Gaussian matched filter (GMF) in combination with the first derivate of a Gaussian (FDOG) was implemented.

The GMF is a two dimensional kernel with a zero mean defined in the x-direction by an inverted Gaussian profile (Fig. 2 b), and in the y-direction by replicates of the same profile (Fig. 2 d). The size of the kernel and corresponding weights is controlled be the standard deviation σ of a constituting Gaussian function defined for $|x| \leq 3\sigma$, $|y| \leq L/2$. The parameters σ and L thereby adjust the filter to match the width and length of the targeted features, respectively.

As illustrated in Fig. 2 c, the GMF yields spurious responses at step edges. This issue can be addressed using an FDOG kernel with the same parameters σ and L (Fig. 2 g, i). As illustrated in Fig. 2 f, the FDOG filter responses have zero crossings at the location of the fissures. When smoothed with a mean filter of the same size as the kernel, the zero crossing yields a plateau with low values for the extent of the fissures. Subtracting the absolute values of the smoothed FDOG response from the GMF response yields the final filter output in which responses are suppressed at step edges (Fig. 2 h, j). For a stronger suppression of edge response, multiples of the FDOG response may be subtracted and the final output can be transferred into a binary response by selecting a threshold according to the desired detection sensitivity. Since in practice the orientation of the fissures is *a priori* unknown, multiple rotated versions of the Gaussian filters are applied to the image and for each pixel only the maximum response value is retained. This corresponds to finding the angle $\theta_{\mathrm{m}}(x, y)$ that maximizes the filter response at a given position in the image $I(x, y)$ using Eq. 1:

$$\theta_{\mathrm{m}}(x, y) = \arg\max_{0<\theta_i \leq \pi}(I(x, y) \otimes GMF_{\theta_i}), \quad (1)$$

where $\otimes$ is the convolution operator and θ_i the orientation of the GMF, for $i = \{1,2, \ldots, 36\}$. The variability of the fissure width also suggests a search among multiple scales, and it has been demonstrated that the family of Gaussian filters provides an adequate framework for scale-space analysis [16]. According to scale-space theory the Gaussian filter will yield a maximum response as it approaches the scale of a target feature present in the image. Applying the filter among a number of predefined scales and retaining for each pixel only the maximum response, this property can be used for automatic scale selection, as recently demonstrated for line detection applications [17]. This is similar to finding the orientation of the fissure and is expressed in Eq. 2:

$$\sigma_{\mathrm{m}}(x, y) = \arg\max_{\sigma_i \in \{0.6, 0.8, \ldots, 3.0\}}(I(x, y) \otimes GMF_{\sigma_i}). \quad (2)$$

In summary, for each pixel the algorithm finds the GMF peak response orientation and scale, calculates the smoothed response of a corresponding FDOG at the same orientation and scale, and subtracts the FDOG from the GMF. All detections were performed on the green band of the image.

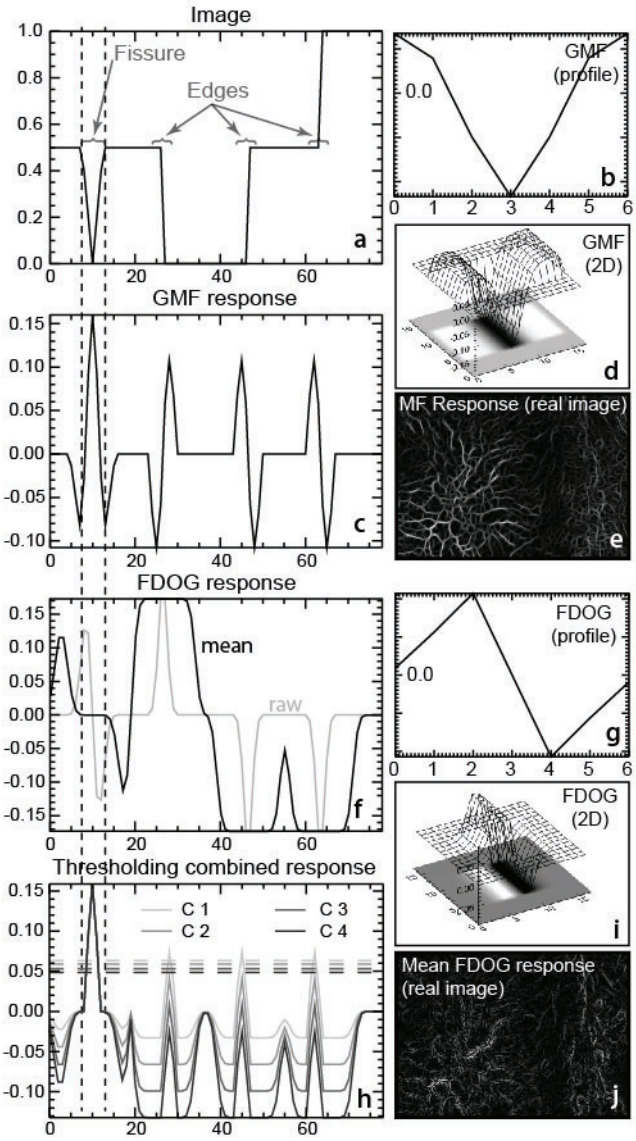

Fig. 2 Illustration of the principles of the Gaussian filtering for a simplified 1-D case (a-c, f-h), a 3D visualization of 2D filters (d, i) and the filter responses on sample image patches (e, j).

3. RESULTS AND DISCUSSION

Receiver operating characteristic (ROC) analysis is a frequently adopted technique to assess the performance of feature detection algorithms since it is not affected by class-imbalance and allows for a threshold independent comparison between different algorithms [18]. A ROC analysis was carried out to assess the performance of the multi-scale fissure detection with respect to two expert maps and compare the results with the single-scale method. Considering a typical length of the targeted fissures of approximately 1 m, the length of the filter was kept constant at $L=12$ pixels for all experiments.

The ROC plots in Fig. 3 d and h illustrate that in most cases the multi-scale algorithm outperforms the single-scale detector, whereas with more conservative thresholds and ground truth (Fig. 3 c) the single-scale detector with the smallest $\sigma=0.6$ still yielded lower false positive rates. This must be attributed to general prevalence of finer fissures and the overall broader responses resulting from peak responses at larger scales in the multi-scale detections. Considering however the less conservative reference image provided by the second operator (Fig. 3 g) the multi-scale detector outperforms also the single-scale detection at $\sigma=0.6$.

In addition to competitive detection accuracies, the proposed algorithm liberates the user from an exhaustive search over all possible scales, and appears especially useful in situations in which the targeted features exhibit great size variability.

A comparison of the manual mappings carried out by two human operators (Fig. 3 c, g) also reveals the uncertainty of the reference data, which is typical among the ground truth maps based on expert judgments. The inter-observer agreement between two human operators still exceeds the accuracy of the automated detection, indicating that, for the specific task, the detector still lacks behind the general performance of human image interpreters, and further enhancements should be possible. However, in order to avoid a focus on individual image interpretations and an eventual reproduction of inherent errors, further efforts should take into account the ground truth uncertainties and agreement among a broader set of image interpreters. For this purpose, reference mappings from multiple human annotators have already been collected, and this is currently being used for further methodological developments and a comprehensive assessment of state-of-the-art crack detection methods in this specific domain.

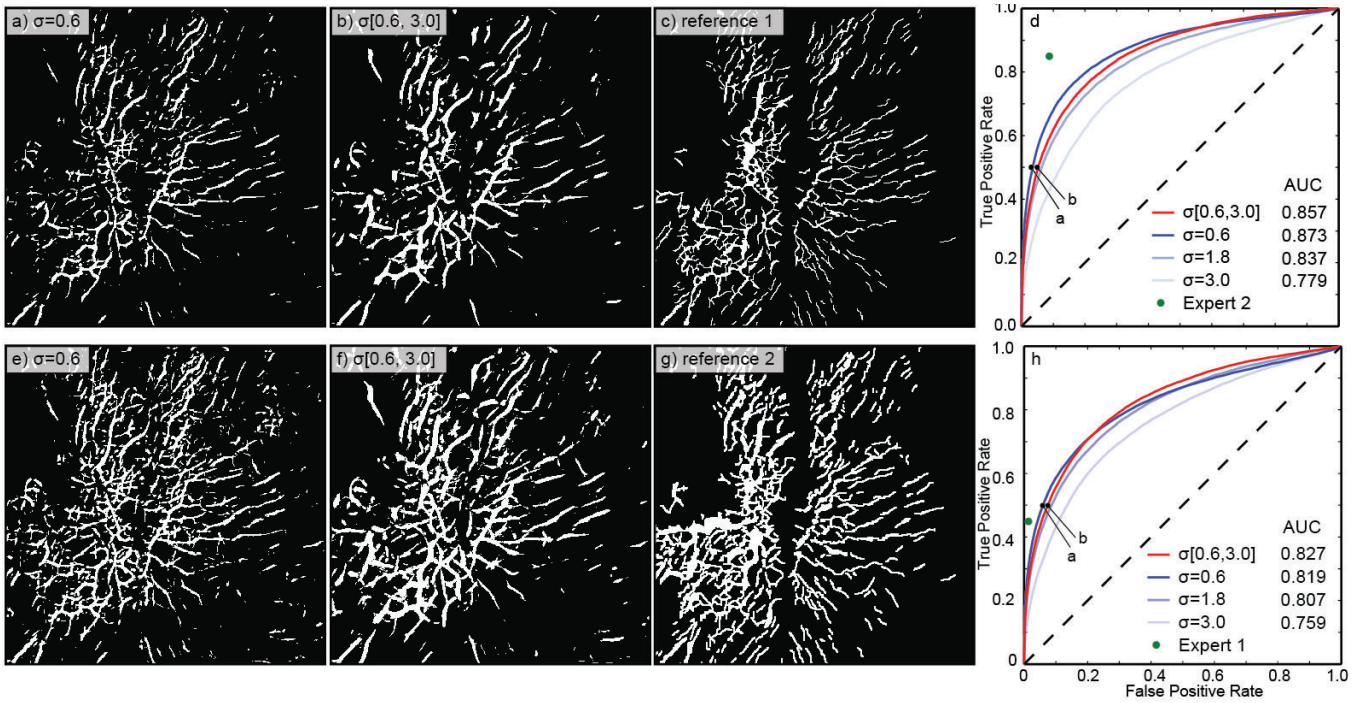

Fig. 3 ROC analysis of single and multi-scale detections (d, h) with two reference datasets (c, g). The best detection results are displayed at a true positive rate of 0.5 (a, b, e, f).

Acknowledgements
The project SafeLand (Grant Agreement No. 226479) funded by the 7th Framework Programme of the European Commission and the project FOSTER funded by the French Research Agency (Contract ANR Cosinus, 2011–2013) supported this work and are thankfully acknowledged.

4. REFERENCES

[1] R. W. Fleming and A. M. Johnson, "Structures associated with strike-slip faults that bound landslide elements," *Engineering Geology,* vol. 27, no. 1–4, pp. 39–114, 1989.

[2] M. Parise, "Observation of surface features on an active landslide, and implications for understanding its history of movement," *Natural Hazards and Earth System Sciences,* vol. 3, pp. 569–580, 2003.

[3] R. N. Chowdhury and S. Zhang, "Tension cracks and slope failure," presented at the Proceedings of the International Conference on Slope Stability Engineering: developments and applications, Isle of Wight, 1991.

[4] G. A. Khattak, L. A. Owen, U. Kamp, and E. L. Harp, "Evolution of earthquake-triggered landslides in the Kashmir Himalaya, northern Pakistan," *Geomorphology,* vol. 115, no. 1–2, pp. 102–108, 2010.

[5] K. B. Krauskopf, S. Feitler, and A. B. Griggs, "Structural Features of a Landslide near Gilroy, California," *The Journal of Geology,* vol. 47, no. 6, pp. 630–648, 1939.

[6] J. P. Malet, T. W. J. van Asch, R. van Beek, and O. Maquaire, "Forecasting the behaviour of complex landslides with a spatially distributed hydrological model," *Natural Hazards and Earth System Sciences,* vol. 5, pp. 71–85, 2005.

[7] U. Niethammer, M. R. James, S. Rothmund, J. Travelletti, and M. Joswig, "UAV-based remote sensing of the Super-Sauze landslide: Evaluation and results," *Engineering Geology,* vol. 128, pp. 2–11, 2011.

[8] L. J. Quackenbush, "A review of techniques for extracting linear features from imagery," *Photogrammetric Engineering & Remote Sensing,* vol. 70, no. 12, pp. 1383–1392, 2004.

[9] G. Papari and N. Petkov, "Edge and line oriented contour detection: State of the art," *Image and Vision Computing,* vol. 29, no. 2–3, pp. 79–103, 2011.

[10] B. V. M. Shruthi, N. Kerle, and V. Jetten, "Object-based gully feature extraction using high resolution imagery," *Geomorphology,* vol. 134, no. 3–4, pp. 260–268, 2011.

[11] A. Baruch and S. Filin, "Detection of gullies in roughly textured terrain using airborne laser scanning data," *ISPRS Journal of Photogrammetry and Remote Sensing,* vol. 66, no. 5, pp. 564–578, 2011.

[12] H. Liu, D. Sherman, and S. Gu, "Automated Extraction of Shorelines from Airborne Light Detection and Ranging Data and Accuracy Assessment Based on Monte Carlo Simulation," *Journal of Coastal Research,* vol. 23, no. 6, pp. 1359–1369, 2007.

[13] A. Stumpf, U. Niethammer, S. Rothmund, A. Mathieu, J.-P. Malet, N. Kerle, and M. Joswig, "Advanced image analysis for automated mapping of landslide surface fissures," presented at the 2nd World Landslide Forum, Rome, 2011.

[14] S. Chaudhuri, S. Chatterjee, N. Katz, M. Nelson, and M. Goldbaum, "Detection of blood vessels in retinal images using two-dimensional matched filters," *IEEE Transactions on Medical Imaging,* vol. 8, no. 3, pp. 263–269, 1989.

[15] B. Zhang, L. Zhang, L. Zhang, and F. Karray, "Retinal vessel extraction by matched filter with first-order derivative of Gaussian," *Computers in Biology and Medicine,* vol. 40, no. 4, pp. 438–445, 2010.

[16] T. Lindeberg, "Feature Detection with Automatic Scale Selection," *International Journal of Computer Vision,* vol. 30, no. 2, pp. 79–116, 1998.

[17] T. A. Lampert and S. E. M. O'Keefe, "A detailed investigation into low-level feature detection in spectrogram images," *Pattern Recognition,* vol. 44, no. 9, pp. 2076–2092, 2011.

[18] T. Fawcett, "An introduction to ROC analysis," *Pattern Recognition Letters,* vol. 27, no. 8, pp. 861–874, 2006.